Switched Beam Antenna Based on RF MEMS SPDT Switch on Quartz Substrate

Shi Cheng, *Student Member, IEEE*, Pekka Rantakari, Robert Malmqvist, *Member, IEEE*, Carl Samuelsson, Tauno Vähä-Heikkilä, *Member, IEEE*, Anders Rydberg, *Member, IEEE*, and Jussi Varis

***Abstract*—This letter demonstrates a 20-GHz radio frequency microelectromechanical system (RF MEMS)-based electrically switchable antenna on a quartz substrate. Two quasi-Yagi antenna elements are monolithically integrated with a single-pole double-throw (SPDT) MEMS switch router network on a 21 mm $\times$ 8 mm chip. Electrical beam steering between two opposite directions is achieved using capacitive MEMS SPDT switches in the router. Port impedance and radiation patterns are studied numerically and experimentally. Measured results show that the switched beam antenna features a 27% impedance bandwidth ($S_{11} = -10$ dB), a gain of 4.6 dBi, and a front-to-back ratio of 14 dB at 20 GHz when the control voltage is applied to one of the switch pairs of the SPDT switch.**

***Index Terms*—Front-to-back ratio, half-power beamwidth (HPBW), quasi-Yagi antenna, radio frequency microelectromechanical system (RF MEMS), single-pole double-throw (SPDT) switch.**

I. Introduction

RECONFIGURABLE antennas using radio frequency microelectromechanical systems (RF MEMS) switches and high-isolation switch circuits have attracted increasing attention from industry and academia in the past decade [1]–[3]. A wide range of applications can be found in such areas as radar systems, reconfigurable wireless communication networks, and space-borne remote sensing.

Compared to p–i–n or field-effect transistor (FET) diode switches, RF MEMS switches offer highly attractive merits, e.g. near-zero power consumption, very high isolation, low insertion loss, high linearity, and low cost [4]. Hence, it is regarded as a promising technology for future reconfigurable microwave and antenna systems, particularly at millimeter-wave frequencies. Using RF MEMS switches, antennas with a variety of reconfigurability in terms of resonance frequency, impedance bandwidth, polarization, and radiation patterns have been recently introduced [5]–[10]. The goal of such reconfigurable apertures is to reduce the system complexity for operation over a wide frequency band or with diverse radiation characteristics. A recent implementation of a switched beam antenna at 24 GHz based on conventional solid-state switches show that such switches represent a large part of the losses [11]. Low-loss RF MEMS switches are, therefore, of great interest to enhance the antenna gain. RF MEMS technology has matured over the years, and it has now reached a level when RF MEMS switches for the first time have been successfully integrated into practical RF systems with proven long-term reliability [12].

This letter presents a 20-GHz two-element array antenna integrated with a single-pole double-throw (SPDT) router based on capacitive RF MEMS switches. Monolithic integration is used in order to avoid interchip connects that usually introduce additional losses at millimeter-wave frequencies. The quasi-Yagi antenna is chosen due to its compact size, sufficient impedance bandwidth, and end-fire radiation patterns [13], [14]. Moreover, such an array antenna is compatible with RF MEMS manufacturing processes. In this letter, the design procedure and numerical analysis of the demonstrated switched beam antenna are described in Section II; the fabricated and experimental verifications are presented in Section III.

II. Quasi-Yagi Antenna and SPDT Switch Designs

A bottom-up approach is employed in the design procedure to reduce the complexity. The quasi-Yagi antenna element and RF-MEMS-based SPDT switch are designed and analyzed individually.

A. Quasi-Yagi Antenna

Fig. 1 depicts the geometry of the quasi-Yagi antenna on a 525-um-thick quartz substrate ($\varepsilon_r = 3.8$ and $\tan\delta = 0.001$). It consists of a dipole-like driven element, a director, and a ground plane. The ground plane acts as a reflector for the antenna. It has negligible effects on the forward gain and large effects on the backward gain and input impedance. The ground size and spacing to the driven element are chosen to be identical to that in the switched beam antenna integrated with the SPDT switch. The driven element is used to adjust the antenna port impedance due to its small effect on the forward gain but large effect on the input impedance. The director is considered the most critical element because of its significant effects on the forward gain, backward gain, and input impedance. The dimensions D_1, L_1, and W remain the same to ensure the antenna elements feature the identical characteristics in the final switchable antenna.

Manuscript received January 17, 2009; revised February 20, 2009. First published March 24, 2009; current version published May 20, 2009. This work was supported in part by the Nordisk Innovations Centre through the project NAME in the Nordic MINT program.

S. Cheng and A. Rydberg are with the Department of Engineering Sciences, Signals and Systems, Uppsala University, 75 121 Uppsala, Sweden (e-mail: shi.cheng@angstrom.uu.se; anders.rydberg@angstrom.uu.se).

P. Rantakari, T. Vähä-Heikkilä, and J. Varis are with Sensing and Wireless Devices, VTT Technical Research Centre of Finland, 02044 Espoo, Finland (e-mail: pekka.rantakari@vtt.fi; tauno.vaha-heikkila@vtt.fi; jussi.varis@vtt.fi).

R. Malmqvist and C. Samuelsson are with the Department of Sensor Technologies, FOI Swedish Defense Research Agency, 58 111 Linköping, Sweden (e-mail: robert.malmqvist@foi.se; carsam@foi.se).

Color versions of one or more of the figures in this letter are available online at http://ieeexplore.ieee.org.

Digital Object Identifier 10.1109/LAWP.2009.2018712

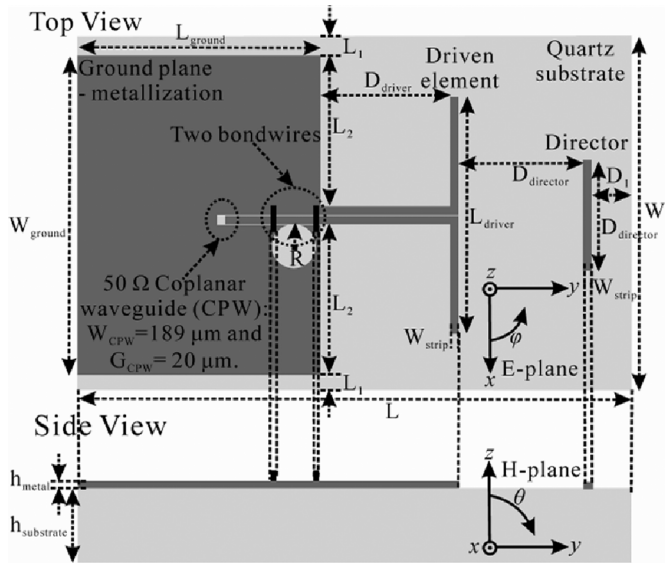

Fig. 1. Geometry of the quasi-Yagi antenna. Dimensions are: $L = 17$ mm, $W = 8$ mm, $L_{\text{ground}} = 5.46$ mm, $W_{\text{ground}} = 7$ mm, $L_{\text{driver}} = 5.35$ mm, $D_{\text{driver}} = 2.91$ mm, $L_{\text{director}} = 2.5$ mm, $D_{\text{director}} = 2.8$ mm, $D_1 = 0.91$ mm, $L_1 = 0.4$ mm, $L_2 = 3.41$ mm, $R = 0.5$ mm, $W_{\text{strip}} = 189\,\mu$m, $h_{\text{metal}} = 1.5\,\mu$m, and $h_{\text{substrate}} = 525\,\mu$m.

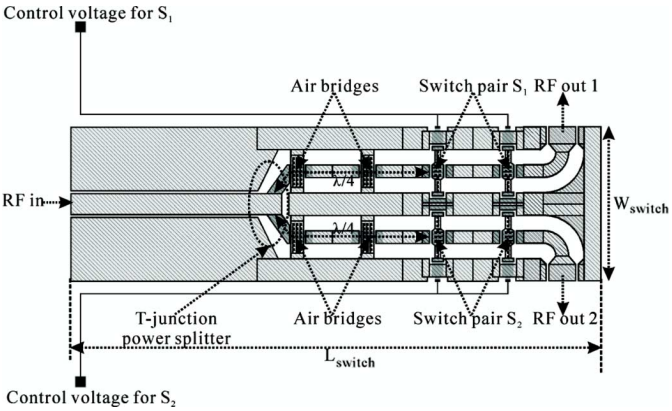

Fig. 2. Layout of the capacitive MEMS SPDT switch. Dimensions are: $L_{\text{switch}} = 3.8$ mm, $W_{\text{switch}} = 1.1$ mm, and λ is the guided wavelength at 20 GHz.

Full-wave simulations using Ansoft HFSS were performed. According to the numerical results on the quasi-Yagi antenna, an impedance bandwidth ($S_{11} = -10$ dB) of 16%, a gain of 5.2 dBi, and a front-to-back ratio of 16 dB can be achieved at 20 GHz.

B. SPDT Switch

Fig. 2 illustrates the layout of the SPDT switch design. The SPDT switch consists of a power splitter and two pairs of capacitive MEMS shunt switches. The MEMS switches are used in pairs to enhance the isolation between the two output ports, and they are at a quarter-wavelength distance from the T-junction at 20 GHz. The quarter-wavelength transmission lines between the T-junction and the switch pairs are capacitively loaded with two air bridges in order to make the SPDT switch more compact in size.

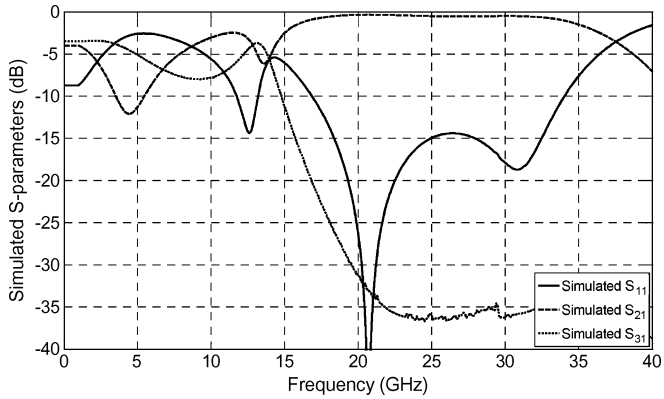

Fig. 3. Simulated S-parameters of the RF-MEMS-based SPDT switch.

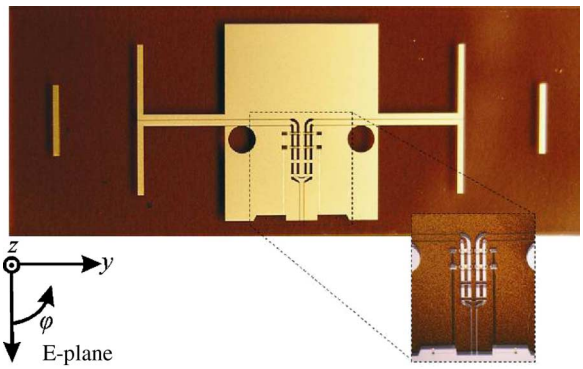

Fig. 4. Photograph of the switched beam antenna integrated with RF-MEMS-based SPDT switch on quartz substrate.

When the control voltage, higher than the pull-in voltage of the MEMS switches, is applied to the switches, the switches close shunting the RF path to the ground. When the switch pair S_1 is open and the S_2 is closed, the RF power flows from the input to the RF out 1 and vice versa.

RF performance of the SPDT switch was numerically analyzed using Sonnet 3D planar electromagnetic software. As shown in Fig. 3, simulated return, isolation, and insertion losses at 20-GHz frequency were 25.3 dB, 31.2, and 0.32 dB, respectively.

III. Experimental Results

The demonstrated prototype was fabricated using a capacitive RF MEMS process at the Ferdinand Braun Kessler (FBK) Institute in Trento, Italy. A photograph of the switched beam antenna integrated with a MEMS switch network is displayed in Fig. 4. The overall size of the quartz chip is 21 mm × 8 mm.

Port impedance and radiation patterns were characterized by applying control voltages with various combinations to the two switch pairs (S_1 and S_2). Fig. 5 shows the measured reflection coefficients of the presented antenna. Experimental results indicate that it achieved an impedance bandwidth ($S_{11} = -10$ dB) of 28% at 20 GHz when either the switch pair S_1 or S_2 was closed.

Figs. 6 and 7 exhibit that the antenna beam can be electrically switched between two opposite directions with a gain of 4.6 dBi,

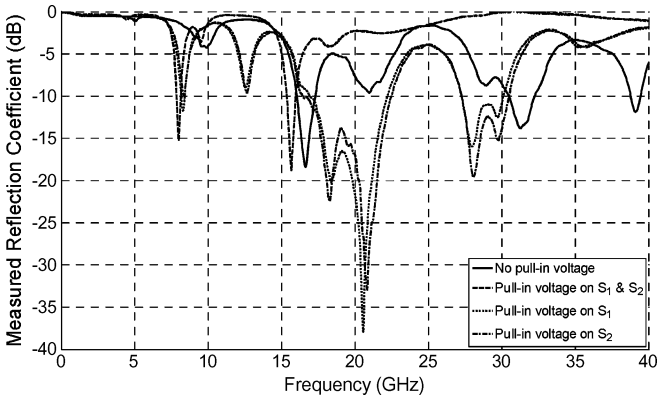

Fig. 5. Measured reflection coefficient of the switched beam antenna integrated with SPDT RF MEMS switch.

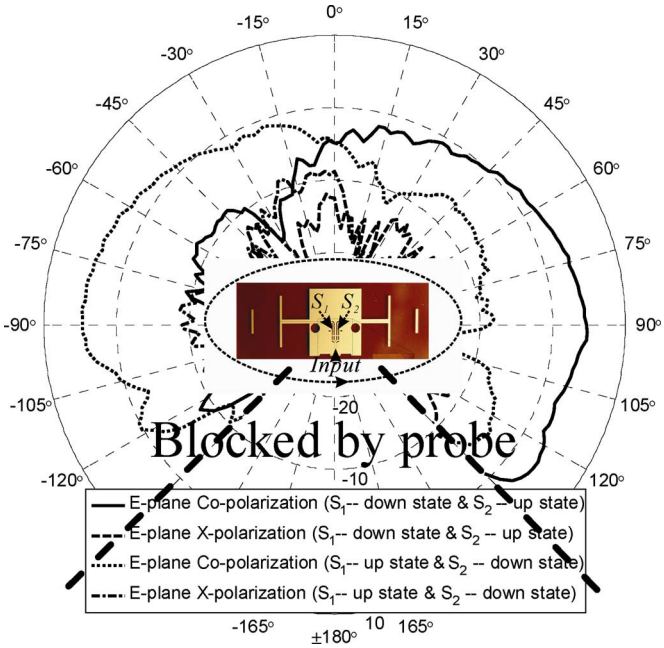

Fig. 6. Measured E-plane radiation patterns (S_1—down-state and S_2—up-state, and S_1—up-state and S_2—down-state).

a half-power beamwidth (HPBW) of 82°, and a front-to-back ratio of 14 dB. Good isolation in the antenna radiation can also be seen while applying the control voltages on both switch pairs. In this case, the radiation decreases 10 dB more than with no control voltages. Moreover, as expected, the cross polarization is much lower than the copolarization in all the experimental results. Ripples can be found in the measured radiation patterns as a result of reflections from the RF probe, dc bias needles, and probe holders. As seen in Fig. 6, radiation is partially blocked due to their presence. As a result of additional losses in the MEMS SPDT switch, the measured gain of the switched beam antenna is 0.6 dB lower than the simulated gain of the single quasi-Yagi antenna element. Compared to MEMS switches, a use of conventional solid-state switches is expected to result in 1-dB higher losses within this frequency range [12]. Therefore, low-loss MEMS switches are essential to obtain a high efficiency for a switched beam antenna.

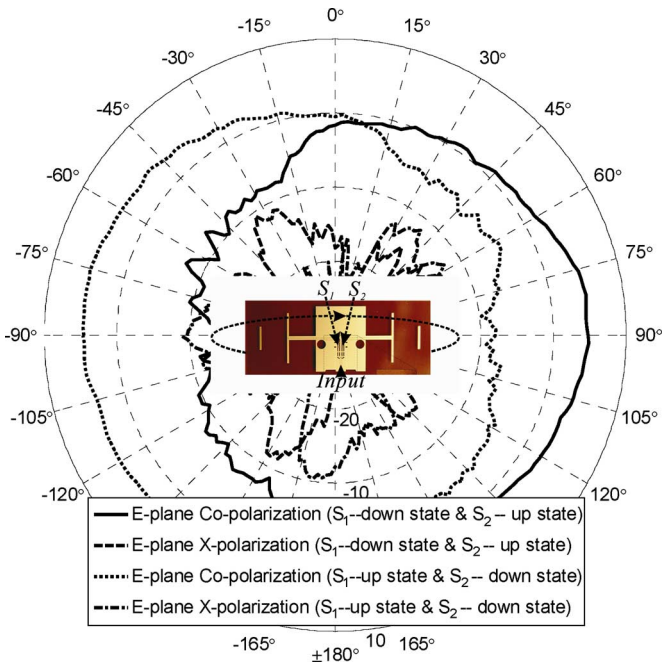

Fig. 7. Measured H-plane radiation patterns (S_1—down-state and S_2—up-state, and S_1—up-state and S_2—down-state).

IV. Conclusion

In this letter, we have presented a 20-GHz switched beam antenna monolithically integrated with a capacitive RF MEMS switch router network on a quartz substrate. The single-chip switched beam antenna features a very compact size as well as good impedance matching and radiation characteristics. Thanks to high isolation of the MEMS switch router and end-fire radiation patterns of the quasi-Yagi antennas, electrical beam switching with highly diverse directivity was achieved. The demonstrated antenna shows that the RF MEMS switch-based router concept works as designed and can be scaled to other frequencies. It can be regarded as a compact and cost-effective solution for certain applications related to wireless communications, sensor networks, automotive radar systems, traffic control, and safety.

References

[1] E. R. Brown, "RF-MEMS switches for reconfigurable integrated circuits," *IEEE Trans. Microw. Theory Tech.*, vol. 46, no. 11, pp. 1868–1880, Nov. 1998.

[2] W. H. Weedon, W. J. Payne, and G. M. Rebeiz, "MEMS-switched reconfigurable antennas," in *Proc. Antennas Propag. Soc. Int. Symp.*, Jul. 2001, vol. 3, pp. 654–657.

[3] C. G. Christodoulou, "RF MEMS and its applications to microwave systems, antennas and wireless communications," in *Proc. IEEE MTT-S Int. Microw. Symp. Dig.*, Sep. 2003, pp. 525–531.

[4] G. M. Rebeiz, *RF MEMS: Theory, Design and Technology*. New York: Wiley, 2003.

[5] D. E. Anagnostou, G. Zheng, M. T. Chryssomallis, J. C. Lyke, G. E. Ponchak, J. Papapolymerou, and C. G. Christodoulou, "Design, fabrication, and measurements of an RF-MEMS-based self-similar reconfigurable antenna," *IEEE Trans. Antennas Propag.*, vol. 54, no. 2, pp. 422–432, Feb. 2006.

[6] K. R. Boyle and P. G. Steenenken, "A five-band reconfigurable PIFA for mobile phones," *IEEE Trans. Antennas Propag.*, vol. 55, no. 11, pp. 3300–3309, Nov. 2006.

[7] C. Jung, M. Lee, G. P. Li, and F. D. Flaviis, "Reconfigurable scan-beam single-arm spiral antenna integrated with RF MEMS switches," *IEEE Trans. Antennas Propag.*, vol. 54, no. 2, pp. 455–463, Feb. 2006.

[8] N. Kingsley, G. E. Ponchak, and J. Papapolymerou, "Reconfigurable RF MEMS phased array antenna integrated within a liquid crystal polymer (LCP) system-on-package," *IEEE Trans. Antennas Propag.*, vol. 56, no. 1, pp. 108–118, Jan. 2008.

[9] K. Topalli, Ö. A. Civi, S. Demir, S. Koc, and T. Akin, "A monolithic phased array using 3-bit distributed RF MEMS phase shifters," *IEEE Trans. Microw. Theory Tech.*, vol. 56, no. 2, pp. 270–277, Feb. 2008.

[10] A. Boe, M. Fryziel, N. Deparis, C. Loyez, N. Rolland, and P. A. Rolland, "Smart antenna based on RF MEMS switches and printed Yagi-Uda antennas for 60 GHz ad hoc WPAN," in *Proc. 36th Eur. Microw. Conf.*, Sep. 2006, vol. 1, pp. 310–313.

[11] P. Hallbjörner, M. Bergstrom, M. Boman, P. Lindberg, E. Öjefors, and A. Rydberg, "Millimetre-wave switched beam antenna using multiple travelling-wave patch arrays," *IEE Proc.-Microw. Antennas Propag.*, vol. 152, no. 6, pp. 551–555, Dec. 2005.

[12] J. J. Maciel, J. F. Slocum, J. K. Smith, and J. Turtle, "MEMS electronically steerable antennas for fire control radars," *IEEE Aerosp. Electron. Syst. Mag.*, vol. 22, no. 11, pp. 17–20, , Nov. 2007.

[13] K. M. K. H. Leong, Y. Qian, and T. Itoh, "First demonstration of a conductor backed coplanar waveguide fed quasi-Yagi antenna," in *Proc. Antennas Propag. Soc. Int. Symp.*, Jul. 2000, vol. 3, pp. 1432–1435.

[14] J. Sor, Y. Qian, and T. Itoh, "Coplanar waveguide fed quasi-Yagi antenna," *Electron. Lett.*, vol. 36, pp. 1–2, Jan. 2000.